Science Advances
AAAS

advances.sciencemag.org/cgi/content/full/5/9/eaar3309/DC1

Supplementary Materials for

Electrode-free nanopore sensing by DiffusiOptoPhysiology

Yuqin Wang, Yu Wang, Xiaoyu Du, Shuanghong Yan, Panke Zhang, Hong-Yuan Chen*, Shuo Huang*

*Corresponding author. Email: shuo.huang@nju.edu.cn (S.H.); hychen@nju.edu.cn (H.-Y.C.)

Published 6 September 2019, *Sci. Adv.* **5**, eaar3309 (2019)
DOI: 10.1126/sciadv.aar3309

The PDF file includes:

Other Supplementary Material for this manuscript includes the following:

(available at advances.sciencemag.org/cgi/content/full/5/9/eaar3309/DC1)

Movie S1 (.mp4 format). Simultaneous imaging of α-HL and ClyA.
Movie S2 (.mp4 format). dsDNA sensing by DOP.
Movie S3 (.mp4 format). Parallel dsDNA sensing by DOP.
Movie S4 (.mp4 format). A single ClyA-RR nanopore inserted in a miniaturized DIB.

Supplementary Methods

Section S1. The FEM simulation

Ca^{2+} binding with the calcium indicator dye Fluo-8 results in fluorescence emission near the pore vicinity. The excessive Ca^{2+}, which binds with EDTA, results in a reduced fluorescence background. These two competing reactions could be described as in **equation (1, 2)**, where α and β stands for the forward and backward binding rate, respectively. The footnote F and E stands for binding with Fluo-8 and EDTA

$$\mathrm{Fluo} + \mathrm{Ca} \overset{\alpha_F, \beta_F}{\longleftrightarrow} \mathrm{FluoCa} \tag{1}$$

$$\mathrm{EDTA} + \mathrm{Ca} \overset{\alpha_E, \beta_E}{\longleftrightarrow} EDTACa \tag{2}$$

Optical single channel recording (oSCR) could be simulated with FEM using the Poisson-Nernst-Planck-Stokes (PNPS) model, where the Nernst-Planck-Stokes equation is described in **equation (3)**

$$D_i \nabla^2 [c_i] + \frac{D_i z_i F}{k_b T} \nabla \cdot ([c_i] \nabla V) + R_i - u \cdot \nabla [c_i] = 0 \tag{3}$$

In the scenario of DiffusiOptoPhysiology (DOP), the electrical potential *V* is set to be constant within the simulation space. **Equation (3)** is thus further simplifiedd (**equation (4)**), where the motion of ions are only driven by passive diffusion, chemical reactions and fluidic flows

$$D_i \nabla^2 [c_i] + R_i - u \cdot \nabla [c_i] = 0 \tag{4}$$

Here, $[c_i]$ starnds for the concentration of different ionic species. R_i stands for chemical reaction terms, u stands for the fluid velocity. Free Ca^{2+} could bind with either Fluo-8 or EDTA as described in **equation (1, 2)**.

For different ions, **equation (4)** is further expanded, where the identity of ions are annotated by the corresponding footnote as described in **equation (5-10)**. Here, FluoCa and EDTACa stands for the bound form of Fluo-8 and EDTA with Ca^{2+}, respectively

$$D_{Fluo}\nabla^2[Fluo] + \beta_F[FluoCa] - \alpha_F[Fluo][Ca^{2+}] - u \cdot \nabla[Fluo] = 0 \quad (5)$$

$$D_{FluoCa}\nabla^2[FluoCa] - \beta_F[FluoCa] + \alpha_F[Fluo][Ca^{2+}] - u \cdot \nabla[FluoCa] = 0 \quad (6)$$

$$D_{EDTA}\nabla^2[EDTA] + \beta_E[EDTA] - \alpha_E[EDTA][Ca^{2+}] - u \cdot \nabla[EDTA] = 0 \quad (7)$$

$$D_{EDTACa}\nabla^2[EDTACa] - \beta_E[EDTACa] + \alpha_E[EDTA][Ca^{2+}] - u \cdot \nabla[EDTA] = 0 \quad (8)$$

$$D_K\nabla^2[K^+] + \frac{D_K z_K F}{k_b T}\nabla \cdot ([K^+]\nabla V) - u \cdot \nabla[K^+] = 0 \quad (9)$$

$$D_{Cl}\nabla^2[Cl^-] + \frac{D_{Cl} z_{Cl} F}{k_b T}\nabla \cdot ([Cl^-]\nabla V) - u \cdot \nabla[Cl^-] = 0 \quad (10)$$

The electrostatic potential in a standard PNPS model is governed by Poisson's equation, which is described in **equation (11)**

$$\nabla^2 V = -\frac{F}{\varepsilon}(z_{Ca}[Ca^{2+}] + z_k[K^+] + z_{Cl}[Cl^-]) \quad (11)$$

However, during DiffusiOptoPhysiology (DOP), the electrical potential V is constant within the simulation space, the equation is thus simplified as **equation (12)**

$$z_{Ca}[Ca^{2+}] + z_k[K^+] + z_{Cl}[Cl^-] = 0 \quad (12)$$

To introduce an osmotic flow across the semi-permeable membrane, a new boundary condition was set on different sides of the membrane by following

$\Delta\pi = (i_{cis}M_{solute,cis} - i_{trans}M_{solute,trans})RT$, where i is the dimensionless van't Hoff index that addresses the number of dissociated ions from each solute molecule, M_{solute} is the molar concentration of the solute, R is the ideal gas constant, and T is the temperature in Kelvins. Here, the positive direction of the osmotic pressure is defined to be from *cis* to *trans*. The osmotic flux is defined as

$$J_v = L_p \Delta\pi \quad (13)$$

where L_p stands for the water permeation constant of the semi-permeable membrane and a value of $10^{-11} m\ Pa^{-1} S^{-1}$ is taken from published literatures[3].

Other simulation parameters are primarily taken from literatures[1]. Here D is the diffusion constant (D_{Fluo}=D_{FluoCa}=15 μm^2 s^{-1}, D_k=D_{cl}=D_{Ca}=D_{EDTA}=D_{EDTACa}=200 μm^2 s^{-1}). z is the charge number (z_{Ca}=+2, z_k=+1, z_{cl}=-1). F is the Faraday constant. k_b is the Boltzmann constant. T is the temperature (300 k). V is the electric potential. α is the forward binding rate ($\alpha_E = 5\ \mu M^{-1}s^{-1}, \alpha_F = 150\ s^{-1}$). β is the backward binding rate ($\beta_E = 0.75\ \mu M^{-1}s^{-1}, \beta_F = 450\ s^{-1}$). The footnote $_E$ and $_F$ stands for EDTA and Fluo-8, respectively. ε is the dielectric constant permittivity of water. The boundary condition on the *cis* side is set with varying KCl concentration (0.5 M to 2.5 M), whereas the boundary condition on *the trans* side is set as 0.75 M $CaCl_2$.

Stationary distribution of ions in different simulation conditions are numerically solved by Comsol 5.3a. Briefly, an axis-symmetric simulation geometry is defined as two hemispherical spaces separated by a semi-permeable membrane, where only the passage of liquid instead of ions are permitted (**Supplementary fig. S1**). The two hemispheres, which represents the *cis* and the *trans* side respectively, are connected by a cylindrical nanopore on the membrane, where free passage of liquid and ions are both permitted.

When illuminated in TIRF mode, the excitation intensity decays exponentially in z-direction. To simulate the fluorescence intensity in a projected x-y plane, **equation (14)** is used, where γ is the decay constant of the evanescent wave in the z direction

$$F(\mathrm{x},\mathrm{y}) = F_0 \int [FluoCa](x,y,z) \exp\left(-\frac{z}{\gamma}\right) dz \quad (14)$$

While the total fluorescence intensity is estimated according to **equation (15)**

$$F_{Total} = \iint F(\mathrm{x},\mathrm{y})\, dxdy \quad (15)$$

Section S2. 2D Gaussian fitting

During DOP recording, the fluorescence intensity profile, which appear as a bright spot, were fit to a 2D Gaussian distribution according to **equation (16)**

$$f(x,y) = z_0 + Aexp\left(-\left(\frac{(x-x_c)^2}{2\sigma_x^2} + \frac{(y-y_c)^2}{2\sigma_y^2}\right)\right) \quad (16)$$

Here, $f(x,y)$ stands for the fitted fluorescence intensity in the x-y plane. z_0 stands for base level, A stands for the fitting amplitude, x_c and y_c stands for the centroid of the fitting. σ_x and σ_y stands for the standard deviation of the distribution in x and y direction, respectively.

This function allows position localization for a tracked spot with sub-pixel resolution. The full width half magnitude (FWHM) of the 2D Gaussian function describes its width at half height and can be used to evaluate the spot size. Here the cftool module in MATLAB is used to perform 2D Gaussian fitting (**Supplementary fig. S5)**. The FWHM were derived from **equation (17)**

$$FWHM = 2\sqrt{2ln2}\sigma_x \quad (17)$$

We defined the pixels within the circle with a diameter of 2 FWHM as the signal, the pixels in the circular ring, between the circles with the diameter of 3 FWHM and 4 FWHM, as background (**Supplementary fig. S5**).

Section S3. SBR evaluation

The SBR value was introduced to quantitatively evaluate the performance of DOP recording from different trials. The SBR value is calculated as

$$SBR = \frac{peak(sig) - mean(bkg)}{std(bkg)} \quad (18)$$

Here, $peak(sig)$ is the peak amplitude $(A + z_0)$ of the signal obtained from 2D Gaussian fitting **(Supplementary fig. S5)**. $mean(bkg)$ is the mean pixel intensity of the background (z_0). $std(bkg)$ is the standard deviation of pixel intensity of the background. The definition of the signal and the background is shown in **Supplementary fig. S5.**

Table S1. $1/\tau_{on}$ and $1/\tau_{off}$ of TriM-β-CD with different [TriM-β-CD]. The DIB was established with 1.5 M KCl, 400 μM EDTA, 40 μM Fluo-8, 10 mM HEPES, pH 7.0 in *cis* and 0.75 M $CaCl_2$, 10 mM HEPES, pH 7.0 in *trans*. TriM-β-CD was added to *cis.* Three independent measurements were performed to form the statistics.

Concentration (mM)	$1/\tau_{on}$ (s^{-1})	$1/\tau_{off}$ (s^{-1})
15	0.027 ± 0.007	2.515 ± 0.440
45	0.047 ± 0.011	2.437 ± 0.449
75	0.086 ± 0.023	2.953 ± 0.616
105	0.127 ± 0.031	3.640 ± 0.330

Table S2. $1/\tau_{on}$ of TriM-β-CD with different [KCl] in cis. The DIB was established with 1-2.5 M KCl, 400 μM EDTA, 40 μM Fluo-8, 10 mM HEPES, pH 7.0 in *cis* and 0.75 M $CaCl_2$, 10 mM HEPES, pH 7.0 in *trans*. 15 mM TriM-β-CD was added to *cis*. Three independent measurements were performed to form the statistics.

KCl concentration (M)	$1/\tau_{on}$ (s^{-1})
1.0	0.056 ± 0.019
1.5	0.028 ± 0.014
2.0	0.023 ± 0.007
2.5	0.022 ± 0.009

Table S3. FWHM and SBR with different [KCl]. The DIB was established with 1-2.5 M KCl, 400 μM EDTA, 40 μM Fluo-8, 10 mM HEPES, pH 7.0 in *cis* and 0.75 M $CaCl_2$, 10 mM HEPES, pH 7.0 in *trans*. Five independent measurements were performed to form the statistics.

KCl concentration(M)	FWHM(μm)	SBR
1.0	2.863 ± 0.156	14.108 ± 3.660
1.5	2.822 ± 0.197	12. 957 ± 2.809
2.0	2.77 ± 0.200	11.228 ± 2.579
2.5	2.65 ± 0.270	6.151 ± 2.295

Table S4. FWHM and SBR with different [$CaCl_2$]. The DIB was established with KCl (0.75 M, 1.5 M and 2.25 M), 400 μM EDTA, 40 μM Fluo-8, 10 mM HEPES, pH 7.0 in *cis* and $CaCl_2$ (0.5M, 1 M and 1.5 M), 10 mM HEPES, pH 7.0 in *trans*. Twelve independent measurements were performed to form the statistics.

$CaCl_2$ concentration(M)	FWHM(μm)	SBR
0.5	2.381 ± 0.376	6.135 ± 3.150
1.0	3.003 ± 0.319	18.482 ± 6.545
1.5	3.888 ± 0.329	24.024 ± 8.304

Table S5. FWHM and SBR of α-HL and ClyA-RR nanopores. The DIB was established with 1.5 M KCl, 400 μM EDTA, 40 μM Fluo-8, 10 mM HEPES, pH 7.0 in *cis* and 1.5 M $CaCl_2$, 10 mM HEPES, pH 7.0 in *trans*. Both types of nanopores were added to *cis*. Five independent measurements were performed to form the statistics.

Type	FWHM(μm)	SBR
α-HL	2.688 ± 0.600	12.24 ± 1.336
ClyA-RR	5.098 ± 0.316	42.893 ± 11.737

Table S6. Nucleic acid abbreviations and sequences.

Abbreviations	Sequences(5'-3')
78 nt ssDNA-a	TTGGCATGTCAGAATGTTAGAATGTTAGAATGTTAGAATGTTAGAAT GTTAGAATGTTTCAGATCTCACTATCAAAAA
78 nt ssDNA-b	TTTTTGATAGTGAGATCTGAAACATTCTAACATTCTAACATTCTAAC ATTCTAACATTCTAACATTCTGACATGCCAA

Note: To form dsDNA, complementary ssDNAs (78 nt ssDNA-a and b) were dissolved in 1.5 M KCl buffer (1.5 M KCl, 10 mM HEPES, pH 7.0), heated up to 95 °C and gradually cooled down (−5 °C/min) to room temperature (25 °C) on a PCR thermal cycler (ABI 2720).

Table S7. Blockade level of dsDNA events. DIB was established with 2.25 M KCl, 400 μM EDTA, 40 μM Fluo-8, 10 mM HEPES, pH 7.0 in *cis* and 1.5 M $CaCl_2$, 10 mM HEPES, pH 7.0 in *trans*. 2 μM dsDNA was added to *cis*. Three independent measurements were performed to form the statistics.

Individual experiments	F_P	τ_{off} (s)
1	0.708	0.136
2	0.653	0.395
3	0.701	0.143

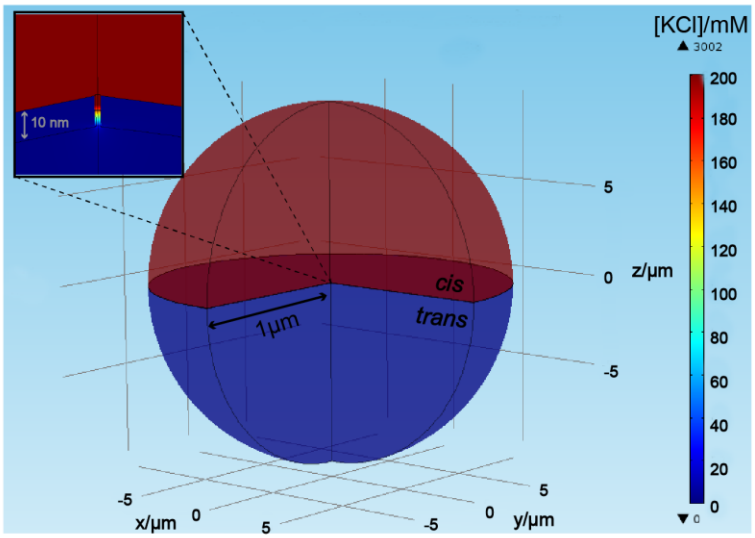

Fig. S1. FEM model geometry. A sphere of 10 µm radius filled with electrolyte solution is separated into two chambers (*cis*: top, *trans*: bottom) by a 10 nm-thick semi-permeable membrane. Only the passage of liquid instead of ions are permitted across the membrane. In the center of the membrane, a single nano-scaled, cylindrical shaped aperture with varying diameter (2 nm-8 nm) is placed, which acts as the only passage for liquid and ion transport between the two chambers. The boundary condition on the *cis* side was set with varying KCl concentrations (1 M to 2.5 M), whereas the boundary condition on the *trans* side was set with varying $CaCl_2$ concentration (0.5 M to 1.5 M). All FEM simulations in this paper were performed using this geometry.

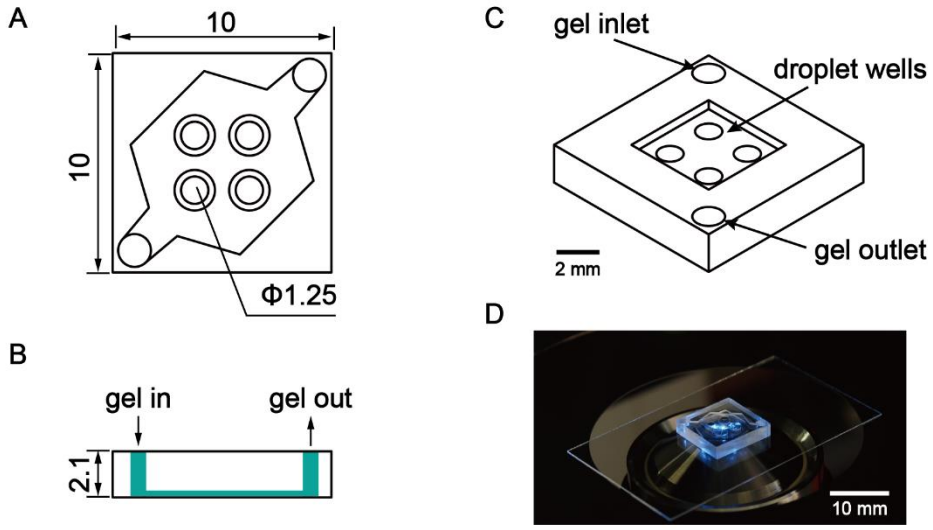

Fig. S2. The DIB device. The PMMA device was custom fabricated. (A) A bottom view of the DIB device used in the experiment. Scale unit: mm. (B) A front view of the DIB device used in the experiment. Scale unit: mm. The molten gel can be infused into the device along the route marked in green. (C) The 3D model of the DIB device. The gel inlet and outlet holes for molten agarose are shown respectively. The gel outlet also helps air bubbles to escape during gel filling. 4 independent droplet wells were designed for parallel measurements. Scale bar: 2 mm. (D) A photograph of a prepared device during DOP recording. The DIB in the setup was excited using a 473 nm laser and imaged using total internal reflection fluorescence (TIRF) microscopy. Scale bar: 10 mm. (Photo credit: Yuqin Wang & Jianbin Pan, School of Chemistry and Chemical Engineering)

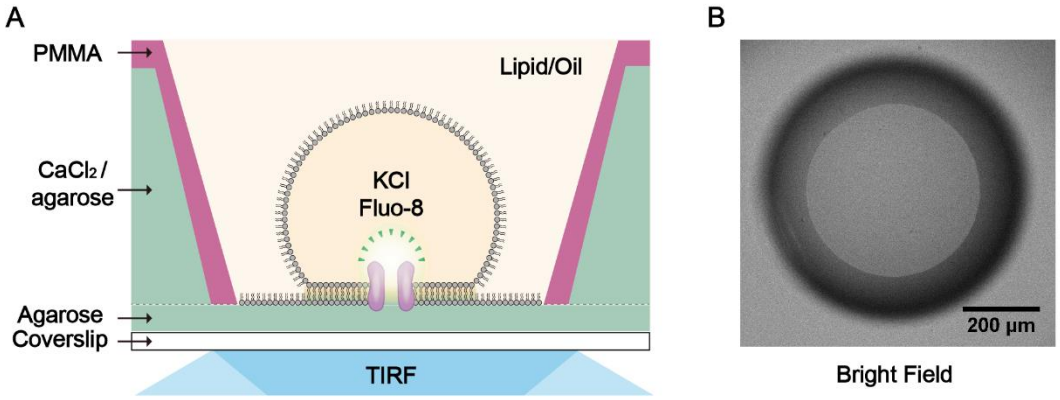

Fig. S3. The schematic diagram of the setup. (A) A cross-sectional view of the setup for DOP recording. When immersed in the lipid/oil environment (2.5 mg/ml DPhPC in the mixture of hexadecane/silicone oil with a 1:1 volume ratio), the aqueous droplet and the agarose substrate spontaneously forms a droplet interface bilayer (DIB) when brought together. The aqueous droplet is composed of 1 M-2.5 M KCl, 400 µM EDTA, 40 µM Fluo-8, 10 mM HEPES, pH 7.0 with biological nanopores. The agarose substrate is composed of 0.5−1.5 M $CaCl_2$, 10 mM HEPES, pH 7.0 with 2.5% (v/w) low melt agarose. Biological nanopores, which were previously dissolved in the droplet, spontaneously insert into the DIB and permits thermodynamic diffusion of Ca^{2+} into the droplet. The transported Ca^{2+}, which immediately bind with Fluo-8 in the droplet, results in fluorescence emission around the pore vicinity when imaged by total internal reflection fluorescence (TIRF) microscopy. (B) A bright-field image of a DIB. The boundary of the DIB is visually resolvable from the bright-field image.

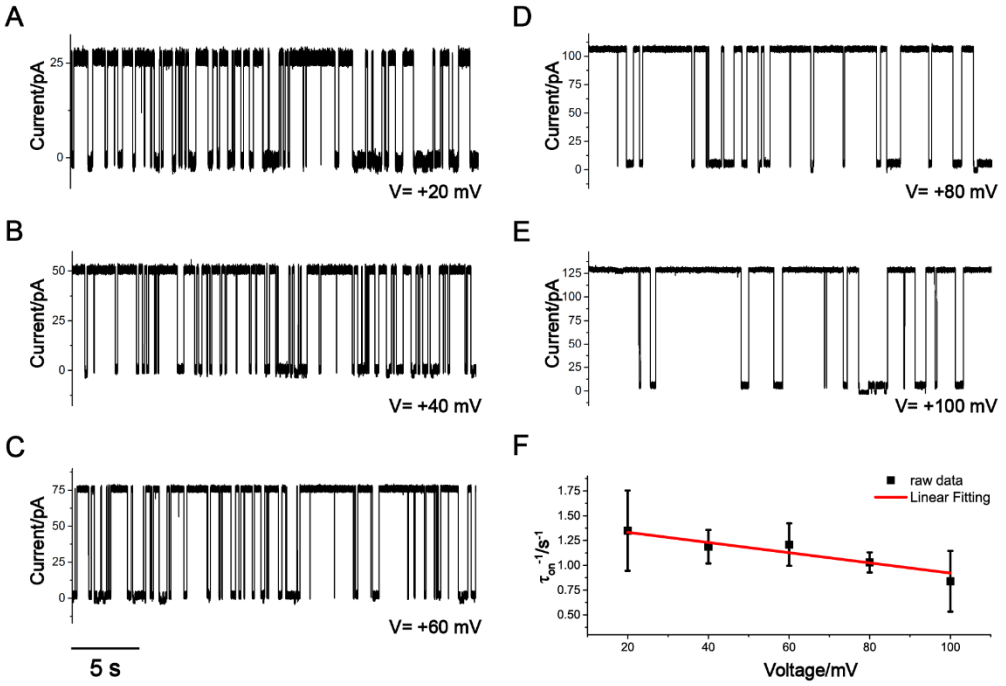

Fig. S4. Cyclodextrin binding kinetics. (A-E) Representative current traces with a +20, +40, +60, +80 and +100 mV applied potential, respectively. Trimethyl-β-cyclodextrin (TriM-β-CD) was added in *cis*, with a final concentration of 4 mM. The event detection frequency systematically decreases when the applied potential increases. This indicates that an opposing electroosmotic flow in the nanopore may exist which has reduced the probability of TriM-β-CD binding with the pore. (F) Plots of $1/\tau_{\mathrm{on}}$ as a function of the applied voltages. The statistics of $1/\tau_{\mathrm{on}}$ was based on three independent sets of electrophysiology recording (N=3) with 90 s duration for each condition. The electrophysiology recordings were performed with 1.5 M KCl, 10 mM HEPES, pH 7.0 in both sides of the membrane. WT α-HL nanopores were added in *cis*.

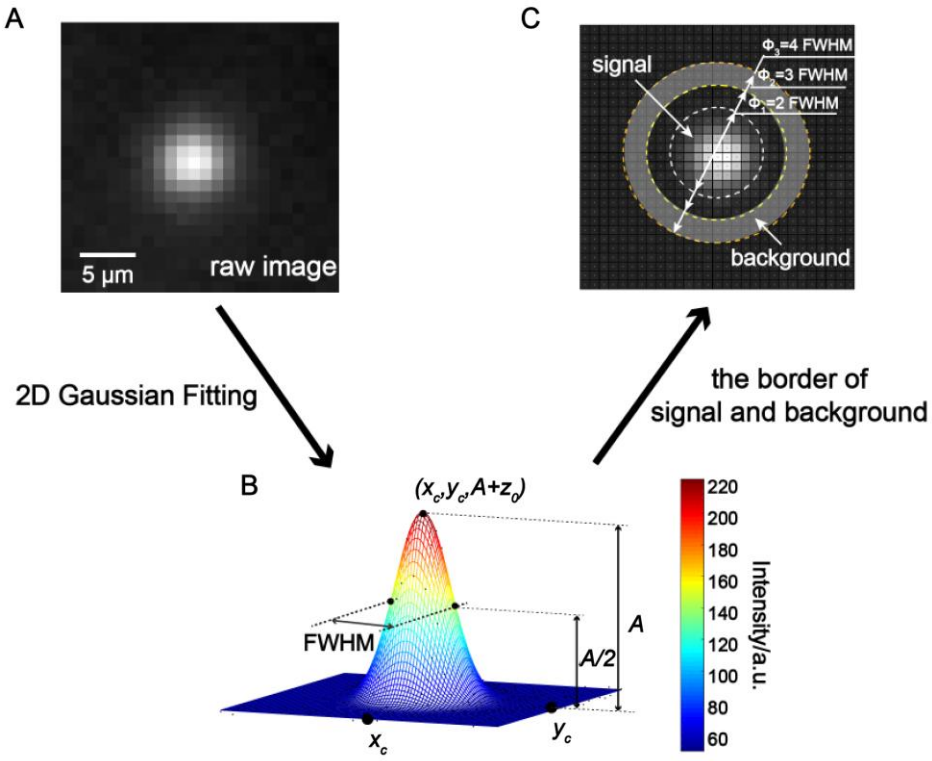

Fig. S5. Definition of signal and background during oSCR. (A) A representative image frame acquired from DOP recording. (B) The 2D Gaussian fitting ($f(x,y) = z_0 + Aexp(-\frac{(x-x_c)^2}{2\sigma_x^2} - \frac{(y-x_c)^2}{2\sigma_y^2})$) result of (A). Parameters such as the center of the peak (x_c,y_c), the peak amplitude ($A + z_0$) and the full width of half maximum (FWHM) can be extracted from the fitting results (**Supplementary Methods 2**). (C) The definition of signal and background according to FWHM. In brief, the total pixel values within the circle with a diameter of 2 FWHM are defined as the signal. The total pixel values within the outer ring, which is between the diameter of 3 FWHM and 4 FWHM, are defined as the background. The demonstrated image processing is automated using MATLAB.

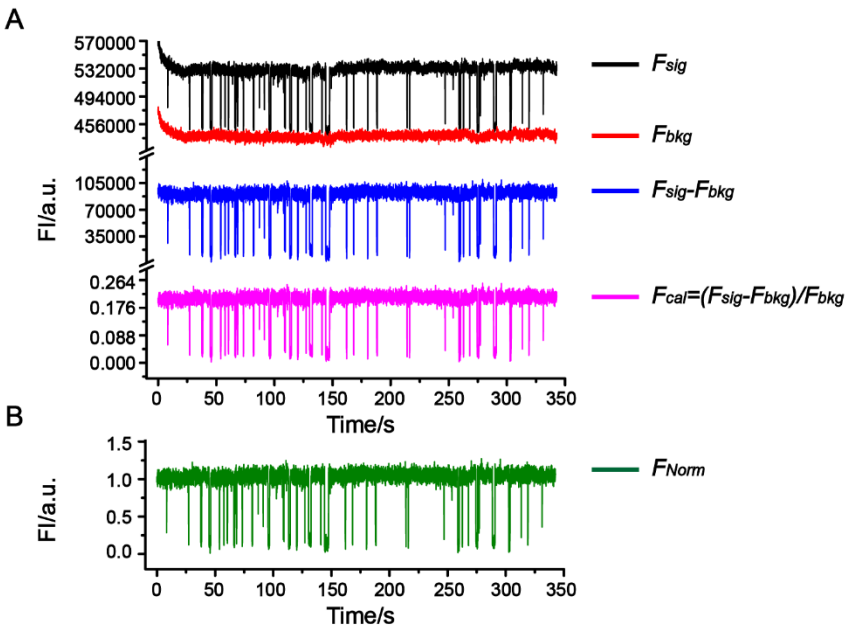

Fig. S6. Demonstration of fluorescence trace normalization. Due to possible power fluctuations from the laser, drift of the focal plane or motion of the nanopore, low frequency fluctuations in the raw fluorescence time trace are sometimes observed. However, these fluctuations could be diminished by standard trace calibration. (A) Calibration of the fluorescence intensities. A sample trace that corresponds to DOP based TriM-β-CD sensing was used as a demonstration **(Fig. 1)**. The raw fluorescence time trace (signal and background) was extracted separately using a custom LabVIEW program. See **Supplementary fig. S5** for the definition of the signal and the background during DOP. Trace calibration is performed according to the formula $F_{cal} = (F_{sig} - F_{bkg})/F_{bkg}$. F_{cal}, F_{sig} and F_{bkg} stands for the calibrated fluorescence intensity, the raw fluorescence signal and the raw fluorescence background respectively. Low frequency fluctuations as observed in the raw fluorescence time trace was minimized after the normalization. (B) The normalized fluorescence time trace. For quantitative analysis, the amplitude of the fluorescence that corresponds to the open pore state is further normalized to be 1.

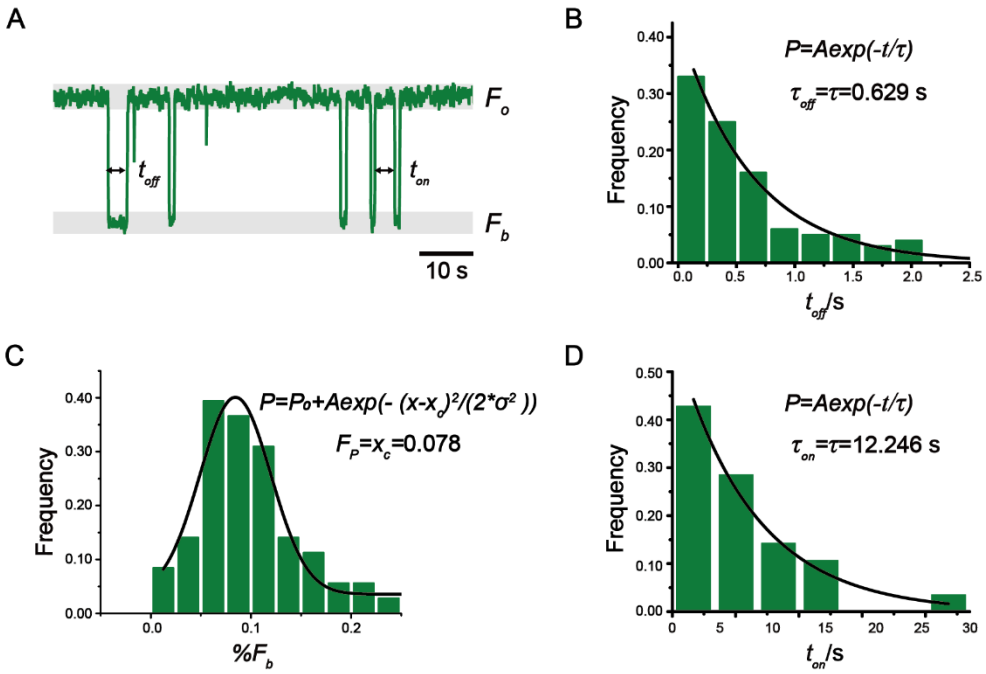

Fig. S7. Event statistics derivation. (A) A representative fluorescence trace showing TriM-β-CD translocation through an α-HL pore. The event dwell time (t_{off}) and the inter-event interval (t_{on}) were defined as marked in the trace. (B) Histogram of the dwell time (t_{off}). The black line is the single exponential fit for the histogram data. The time constant τ_{off} was derived from the fitting results. (C) Histogram of the percentage blockade depth (%F_b). The peak value x_c is defined as the mean blockage depth F_P. (D) Histogram of the inter-event intervals (t_{on}). The black line is the single exponential fit for the histogram data. The time constant τ_{on} was derived from the fitting results.

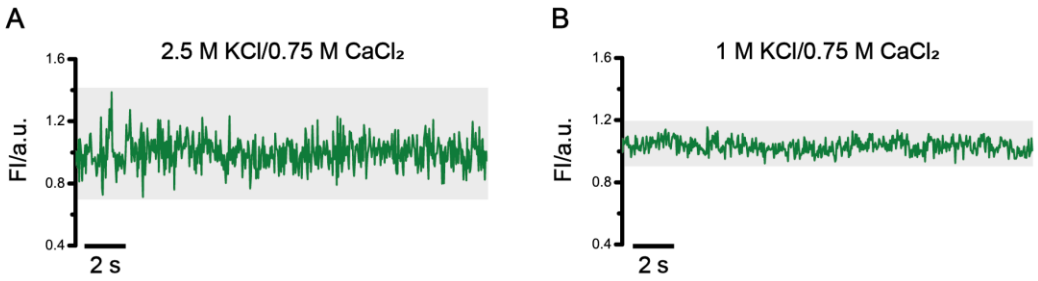

Fig. S8. Baseline comparison during TriM-β-CD sensing. (A) A representative fluorescence trace from DOP recording, acquired with 2.5 M KCl, 400 μM EDTA, 40 μM Fluo-8, 15 mM TriM-β-CD, 10 mM HEPES, pH=7.0 in *cis* and 0.75 M $CaCl_2$, 10mM HEPES (pH=7.0) in *trans*. (B) A representative fluorescence trace from DOP recording, acquired with 1 M KCl, 400 μM EDTA, 40 μM Fluo-8, 15 mM TriM-β-CD, 10 mM HEPES (pH=7.0) in cis and 0.75 M $CaCl_2$, 10mM HEPES, pH=7.0 in trans. Both traces were recorded by DOP recording from an α-HL nanopore. The reduction of thermal noises, which results from the enhancement of the absolute fluorescence intensity during DOP recording, was observed when an osmotic flow from *cis* to *trans* exists.

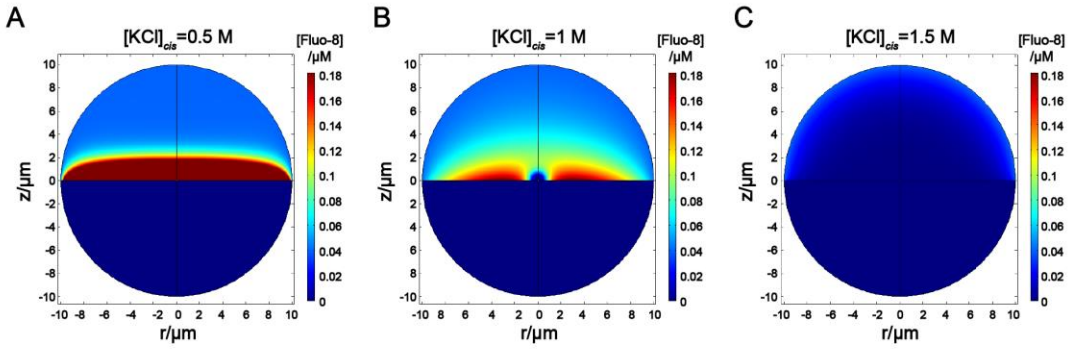

Fig. S9. FEM modeling of Fluo-8 distribution. The Fluo-8H placed in *cis* is a cell-impermeant derivative of Fluo-8 (AAT bioquest). Osmotic flow of water across the membrane results in the enrichment of Fluo-8 around the *cis* side of the DIB. This phenomenon should contribute to the enhanced SBR of nanopore fluorescence when the electrolyte osmolarity in *cis* was set lower than that in *trans*. The Fluo-8 concentration was simulated using FEM modelling **(Supplementary Methods)**. For all simulations, the concentration of KCl, EDTA and Fluo-8 on the *cis* boundary was set to be 0.5-1.5 M, 400 μM and 40 μM, respectively. The concentration of $CaCl_2$ on the *trans* boundary was kept constant at 0.75 M. These simulation parameters, which were set on the boundary of the simulation space, represent the steady state of the electrolyte buffer that is distant away from the nanopore. (A) A cross-sectional view of the 3D distribution of Fluo-8 when the KCl concentration on the *cis* boundary is 0.5 M. Strong osmotic flow from *cis* to *trans* exists in this situation, which results in the enrichment of Fluo-8 near the membrane. (B) A cross-sectional view of the 3D distribution of Fluo-8 when the KCl concentration on the *cis* boundary is 1 M. A decreased enrichment of Fluo-8 is observed. (C) A cross-sectional view of the 3D distribution of Fluo-8 when the KCl concentration on the *cis* boundary is 1.5 M. Weak osmotic flow from *trans* to *cis* exists in this condition, which results in a reduced Fluo-8 concentration near the membrane.

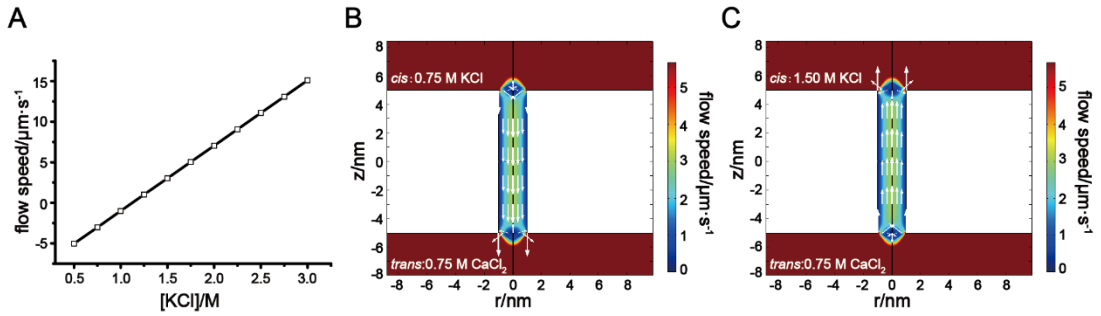

Fig. S10. FEM modeling of the osmotic flow. The boundary conditions on the *cis* side, such as the concentration of KCl, EDTA and Fluo-8 was set to be 0.5-3.0 M, 400 μM and 40 μM respectively. Whereas, the boundary conditions on the *trans* side, such as the concentration of $CaCl_2$, was kept at 0.75 M. The pore, which has a cylindrical geometry, is set to have a diameter of 2 nm. (A) A plot of the flow speed at the center of the pore versus different KCl concentrations in *cis*. (B) A cross-sectional view of the osmotic flow in the pore when the KCl concentrations set on the cis boundary is 0.75 M. In this condition, an osmotic flow is established which directs from *cis* to *trans* (marked with white arrows). (C) A cross-sectional view of the osmotic flow in the pore when the KCl concentration set on the *cis* boundary is 1.50 M. In this condition, an osmotic flow is established which directs from *trans* to *cis* (marked with white arrows).

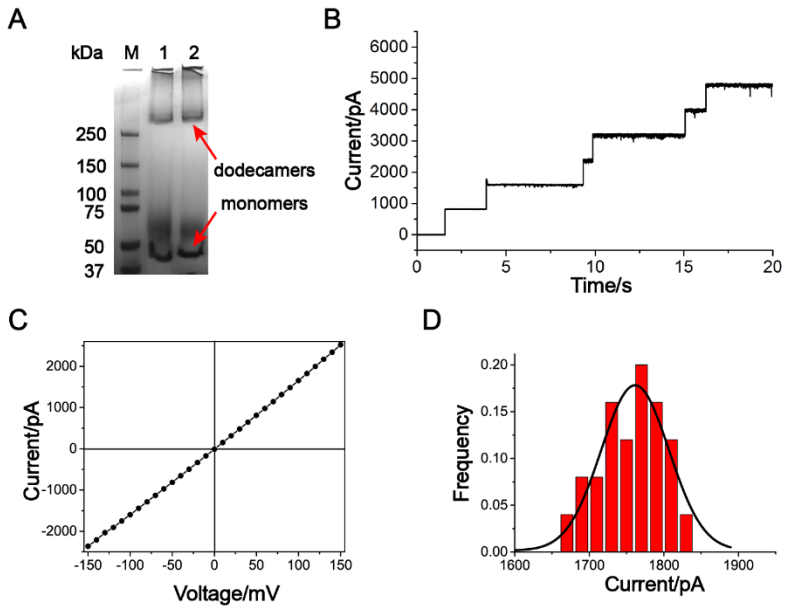

Fig. S11. The preparation and characterization of ClyA-RR. (A) Dodecameric ClyA-RR characterized using blue native gel electrophoresis (4-15% polyacrylamide gradient gel). Lanes M: precision plus protein standards (Bio-Rad); Lane 1: ClyA-RR prepared using prokaryotic expression. Lane 2: ClyA-RR after the addition of DDM, reaching a final concentration of 0.25% (w/v). The gel results showed that the oligomerization of ClyA was formed before the addition of DDM. However, to strictly follow published protocols (**Materials and Methods**), ClyA nanopores used in this study were all prepared with the addition of DDM. (B) Continuous channel insertions by ClyA-RR nanopores were observed during electrophysiology recording. The measurement was carried out with a +50 mV constant voltage. Dodecameric ClyA-RR nanopores were added in *cis*. (C) A representative I-V curve of a ClyA-RR nanopore. (D) The open pore current histogram of ClyA-RR with a +100 mV applied potential. The current was centered at 1761.428 pA. The statistics of open pore current was based on 20 independent sets of electrophysiology recordings (N=20). All demonstrated measurements (B-D) were carried out with 1.5 M KCl, 10 mM HEPES, pH 7.0 in both chambers.

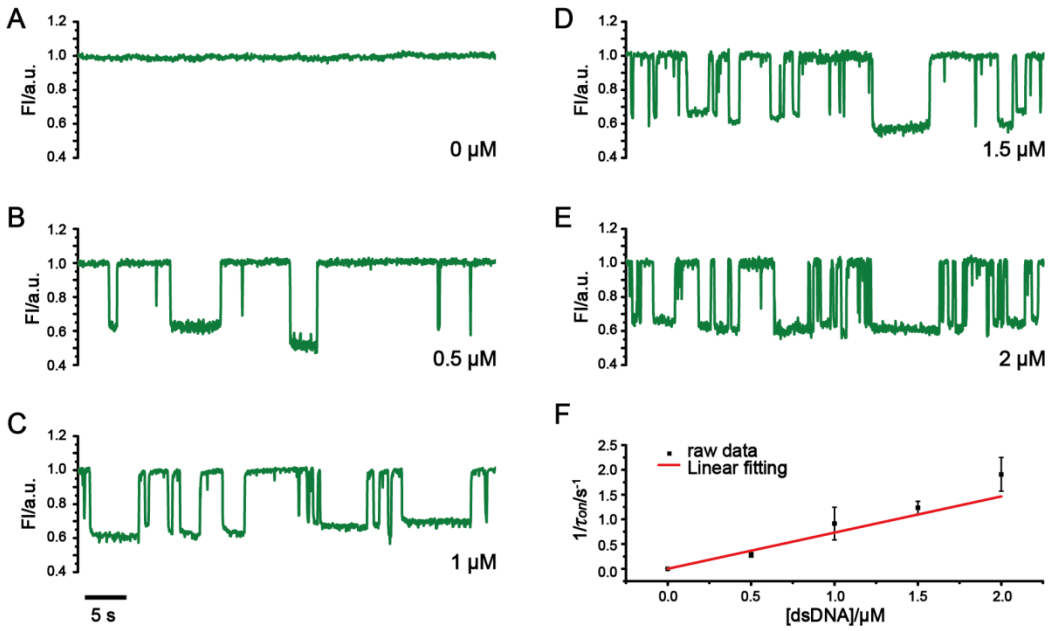

Fig. S12. Observing dsDNA events with different dsDNA concentrations.

Representative Fluorescence traces from a single ClyA-RR nanopore when 0 (A), 0.5 (B), 1 (C), 1.5 (D) or 2 μM (E) dsDNA was added in droplets respectively. The rate that blockade events could be observed increases when the concentration of dsDNA in the droplet is increased. (F) Plots of $1/\tau_{on}$ as a function of the dsDNA concentration. The statistics of $1/\tau_{on}$ was based on three independent sets of DOP recordings (N=3) for each condition. The DOP recordings were performed with 2.25 M KCl, 400 μM EDTA, 40 μM Fluo-8, 10 mM HEPES, pH 7.0 in *cis* and 1.5 M $CaCl_2$, 10 mM HEPES, pH 7.0 in *trans*.

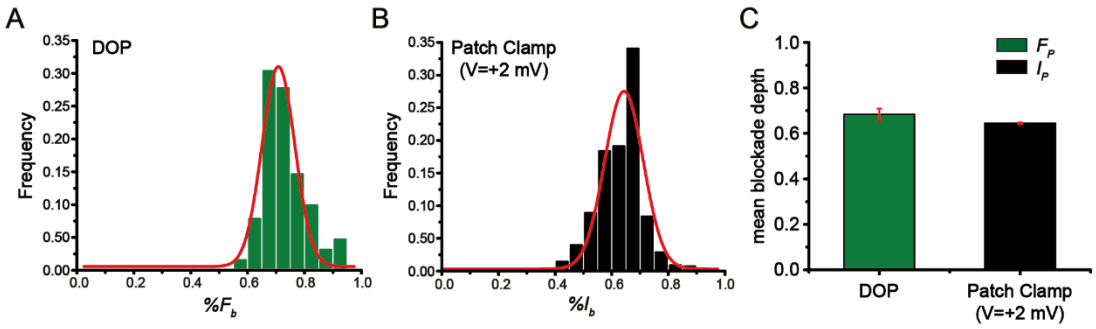

Fig. S13. Statistics of dsDNA events acquired from ClyA-RR. (A) Statistics of % fluorescence blockade level ($\%F_b$) from dsDNA events acquired by DOP. The value of F_P, which was derived from the Gaussian fitting, is 0.708 ± 0.004 (center value ± FWHM). (B) Statistics of % current blockade level ($\%I_b$) from dsDNA events acquired by electrophysiology with a +2 mV applied potential. The value of I_P, which was derived from the Gaussian fitting, is 0.644 ± 0.007. (C) Mean blockade depth comparison between electrophysiology and DOP. The mean blockade depth (the F_p from DOP or the I_p from electrophysiology) appear similar in amplitude. The DOP recordings were acquired with 2.25 M KCl, 400 μM EDTA, 40 μM Fluo-8, 15 mM TriM-β-CD, 10 mM HEPES pH=7.0 in *cis* and 1.5 M $CaCl_2$, 10 mM HEPES, pH=7.0 in *trans*. The electrophysiology recordings were carried out with 2.25 M KCl, 10 mM HEPES, pH 7.0 in *cis* and 1.5 M $CaCl_2$, 10 mM HEPES, pH 7.0 in *trans*. 2 mM 78 bp dsDNA was added in *cis*. Nanopores used in both studies are ClyA-RR.

Movie S1. Simultaneous imaging of α-HL and ClyA. A DIB was established (**Supplementary fig. S2**) between a micro-droplet (~200 nL, *cis*: 1.5 M KCl, 10 mM HEPES, heptameric α-HL WT, dodecameric ClyA-RR, 40 μM Fluo-8H, 400 μM EDTA, pH: 7.0) and a thin layer of hydrogel (~100 nm in thickness, *trans*: 1.5 M $CaCl_2$, 10 mM HEPES, pH: 7.0). Spontaneous insertions from α-HL and ClyA nanopores within the DIB results in the appearance of fluorescence spots of distinct sizes and intensities of fluorescence. Due to a significantly larger pore restriction, the fluorescence from ClyA-RR (marked with red circles) are much brighter than that from α-HL (marked with yellow circles) within the same field of view.

Movie S2. dsDNA sensing by DOP. A DIB was established (**Supplementary fig. S2**) between a micro-droplet (~200 nL in volume, *cis*: 2.25 M KCl ,10 mM HEPES, 2 mM 78-bp dsDNA, dodecameric ClyA RR, 40 μM Fluo-8H, 400 μM EDTA, pH: 7.0) and a thin layer of hydrogel (~100 nm in thickness, *trans*: 1.5 M $CaCl_2$, 10 mM HEPES, pH: 7.0). An inserted ClyA nanopore within the DIB results in the appearance of a bright fluorescence spot (left in the video, Scale bar: 5 μm) when imaged by TIRF microscopy (**Methods**). Frequent resistive pulses were observed via the extracted fluorescence trace (right in the video). The observed resistive pulses result from dsDNA interaction with the ClyA nanopore.

Movie S3. Parallel dsDNA sensing by DOP. A DIB was established (**Supplementary fig. S2**) between a micro-droplet (~200 nL in volume*, cis*: 2.25 M KCl ,10 mM HEPES, 2 mM 78-bp dsDNA, dodecameric ClyA RR, 40 μM Fluo-8H, 400 μM EDTA, pH: 7.0) and a thin layer of hydrogel (~100 nm in thickness, *trans*: 1.5 M $CaCl_2$, 10 mM HEPES, pH: 7.0). ClyA-RR nanopores, which were placed in *cis*, spontaneously insert into the DIB and appear as bright fluorescent spots during DOP recording. The region of interest, which contains two ClyA-RR nanopores in the DIB (Scale bar: 5 μm) were imaged by TIRF microscopy (**Methods**). Events of dsDNA induced pore blockades were observed in parallel from both pores, which appear as spontaneous reduction and recovery in the fluorescence intensity.

Movie S4. A single ClyA-RR nanopore inserted in a miniaturized DIB. A miniaturized DIB was established (**Supplementary fig. S2**) between a micro-droplet (~30 pL in volume, *cis*: 1.5 M KCl, 10 mM HEPES, dodecameric ClyA-RR, 40 μM Fluo-8H, 400 μM EDTA, pH: 7.0) and a thin layer of hydrogel coating (~100 nm in thickness, *trans*: 1.5 M $CaCl_2$, 10 mM HEPES, pH: 7.0). The bright fluorescent spot in the center of the video results from an inserted ClyA-RR nanopore within this mini-DIB when imaged by TIRF microscopy. The fluorescence intensity of the spot stays stable for ~10 minutes.